SUPPORTING INFORMATION

In situ SEIRAS analysis of enhanced photocatalytic carrier transfer to Pt cocatalyst induced by sacrificial reagents

Shu Ashimura,[a] Ota Mori,[a] Reiya Konaka,[a] Takuya Iwai,[a] Chechia Hu,[b] Ke-Hsuan Wang,[c] Chien-Hsiang Chang,[d] Yuh-Lang Lee,[d] and Masaaki Yoshida*[,a,e]

[a] *Yamaguchi University, 2-16-1, Tokiwadai, Ube, Yamaguchi 755-8611, Japan*

[b] *National Taiwan University of Science and Technology, Daan Dist., Taipei City 106, Taiwan*

[c] *Sanyo-Onoda City University, 1-1-1, Sanyo-Onoda, Yamaguchi 756-0884, Japan*

[d] *National Cheng Kung University, No. 1, University Road, Tainan 70101, Taiwan*

[e] *Blue Energy Center for SGE Technology (BEST) of Yamaguchi University*

E-mail: yoshida3@yamaguchi-u.ac.jp

Index **Page**

Experimental methods

Preparation of samples. An anatase-type TiO_2 photocatalyst (Kanto Chem.) with photodeposited Pt particles was prepared using the following procedure. A quantity of the TiO_2 (5 mg) was first suspended in a mixture of 270 µl ultrapure water and 30 µl ethanol. This suspension was then dropped onto a silicon prism (20 mm × 15 mm × 9 mm, Pier Optics) and sintered by heating from room temperature to 300 °C at a rate of 2 °C/min, followed by a hold at 300 °C for 1 h. Finally, Pt/TiO_2 containing 10 wt% Pt was prepared by dropping an aqueous $H_2PtCl_6 \cdot H_2O$ solution (Fujifilm Wako Pure Chemical, 19.3 mM) onto the prism followed by irradiation with a UV light emitting diode (ULEDN-101, NS Lighting). The resulting photocatalyst was characterized using transmission electron microscopy (TEM, JEM-2100PLUS, JEOL), energy-dispersive X-ray spectroscopy (EDX, JED-2300, JEOL), X-ray photoelectron spectroscopy (XPS, K-Alpha, Thermo Scientific), X-ray diffraction (XRD, Ultima IV Protectus, Rigaku) and X-ray absorption fine structure (XAFS) analyses. Pt wire (Nilaco) and PtO_2 powder (Wako) were used as references for the XPS assessments.

Pt-L_3 edge XAFS data were acquired at the BL01B1 and BL-9A beamlines within the SPring-8 and KEK-PF facilities, respectively, using methods similar to those described in a previous paper.[1-3] The Pt foil reference spectrum was obtained in transmission mode with the photon energy calibrated based on the first peak maximum of the first derivative spectrum at 11,564 eV.[4] Spectra of the Pt/TiO_2 samples and the PtO_2 reference were generated in the fluorescence mode using a 19-element Ge detector equipped with a Ga filter and soller slits. The raw XAFS spectra were analysed using the Athena/Artemis software.[5-7]

Photocatalytic properties. The Pt/TiO_2 photocatalysts were evaluated by performing the hydrogen evolution reaction in a reactor filled with Ar gas. This procedure employed three different sacrificial agents, each with varying reducing power: ultrapure water, 15 vol% (2.5 M) ethanol (Shimakyu's Pure Chemicals, ≥99.5%) or 15 vol% (3.7 M) methanol (Honeywell, 99.9%). A 400 W metal halide lamp (10^{-1} mW/cm^2) (HPA400, Phillips, λ_{max} = 360 nm) was used and the amount of hydrogen evolved was measured by injecting the gas resulting from the reaction into a gas chromatograph (GC-2014, Shimadzu) using Ar as the carrier gas. The extent of hydrogen evolution was evaluated at 30 min intervals to assess hydrogen evolution over time.

Surface morphology and particle size distribution diagram of Pt/TiO_2 photocatalysts

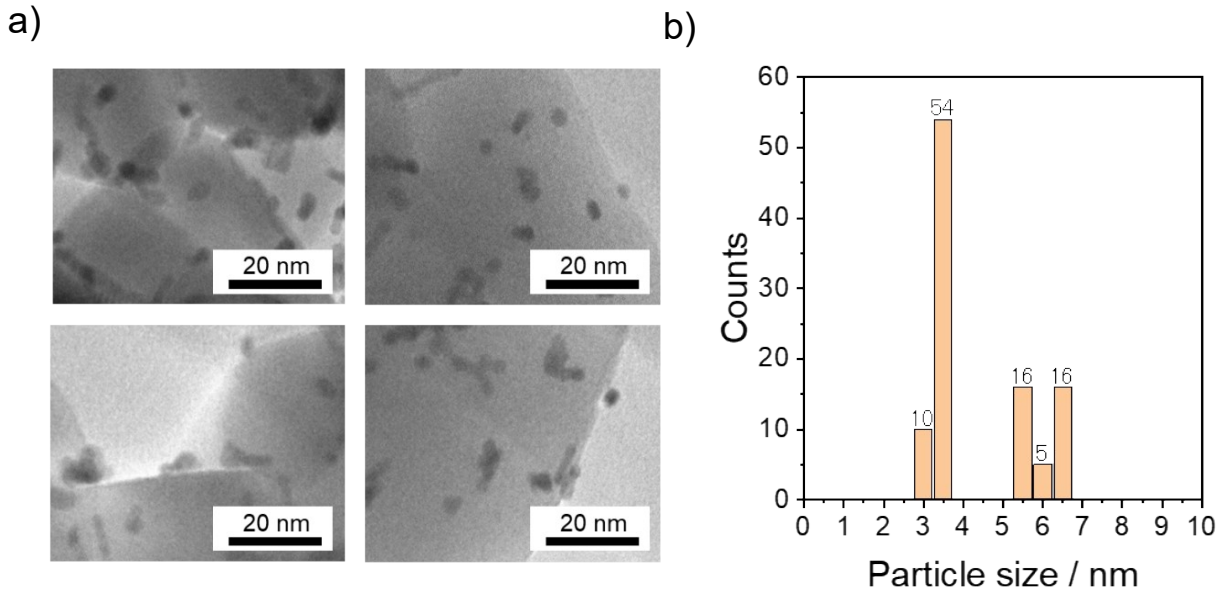

Fig. S1 a) TEM images of Pt nanoparticles ranging in size from several to approximately 10 nm photodeposited on TiO_2 photocatalyst. b) Particle size distribution diagram of Pt cocatalyst photodeposited on TiO_2 photocatalyst. The figure shows the particle size of each Pt particle obtained from TEM images. The numbers on the bar graph represent the number of particles. The average particle size was roughly estimated as 4.4 nm.

Structural state of Pt/TiO_2 photocatalyst

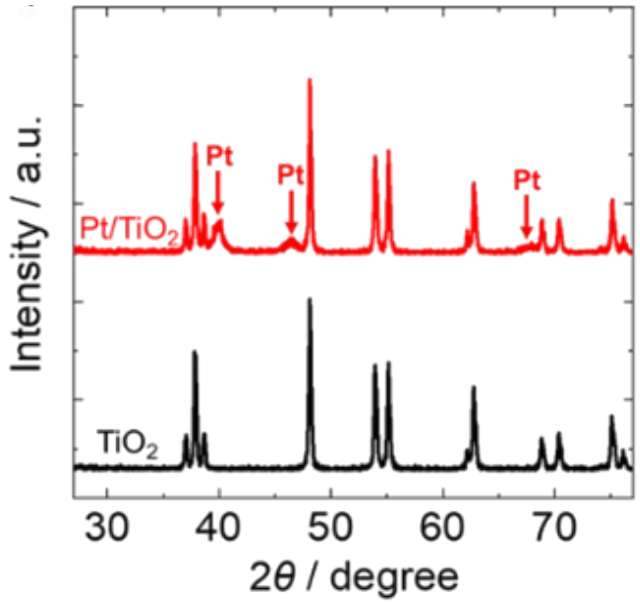

Fig. S2 XRD patterns for TiO_2 before (black line) and after (red line) Pt photodeposition. The diffraction peaks originating from anatase TiO_2 were retained following the photodeposition and new peaks attributed to the (111), (200) and (220) planes of Pt appeared at 40.0°, 46.4° and 67.7°, respectively.

Elemental composition of Pt/TiO_2 photocatalyst

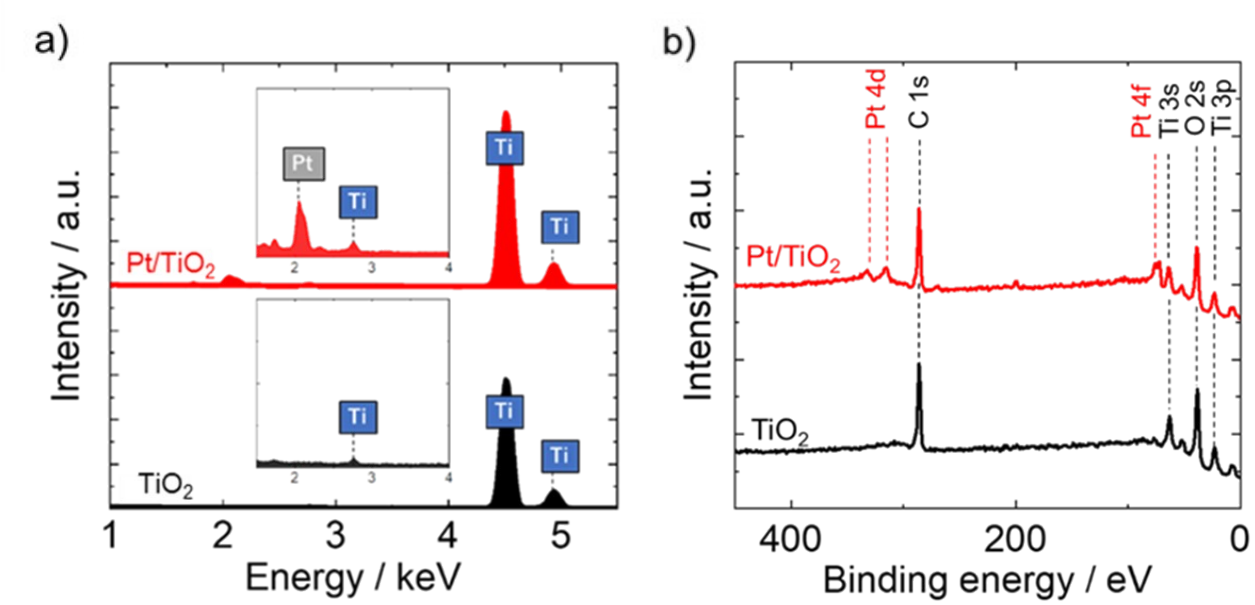

Fig. S3 a) EDS spectra and b) wide-scan XPS spectra of Pt/TiO_2 photocatalyst and of original TiO_2. In both, peaks corresponding to Ti and Pt are evident, confirming that Pt particles were photodeposited on the TiO_2 photocatalyst.

Chemical state of Pt cocatalyst on TiO_2

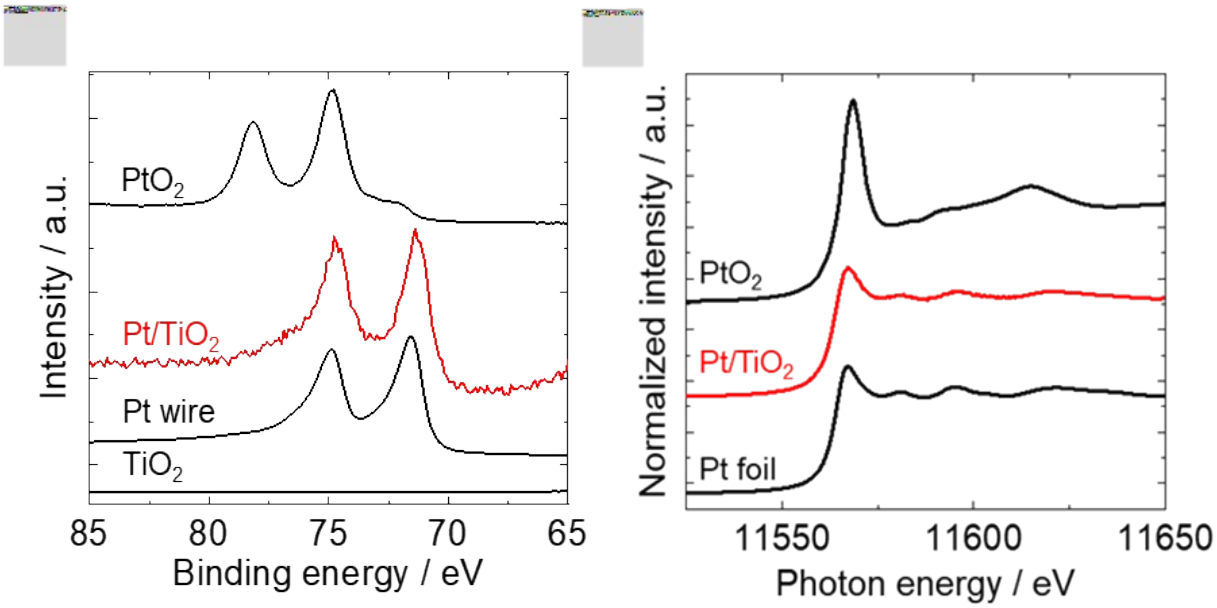

Fig. S4 a) Narrow-scan Pt 4f XPS spectra acquired from Pt/TiO_2 photocatalyst, original TiO_2, PtO_2 and Pt wire. b) Pt L_3-edge XAFS spectra of Pt/TiO_2 photocatalyst, PtO_2 and Pt foil. The Pt/TiO_2 spectra match those of the Pt metal reference material, suggested that the Pt cocatalyst on the TiO_2 was in a metallic state.

Structural analysis of Pt/TiO_2 photocatalyst by curve-fitting of FT-EXAFS spectrum

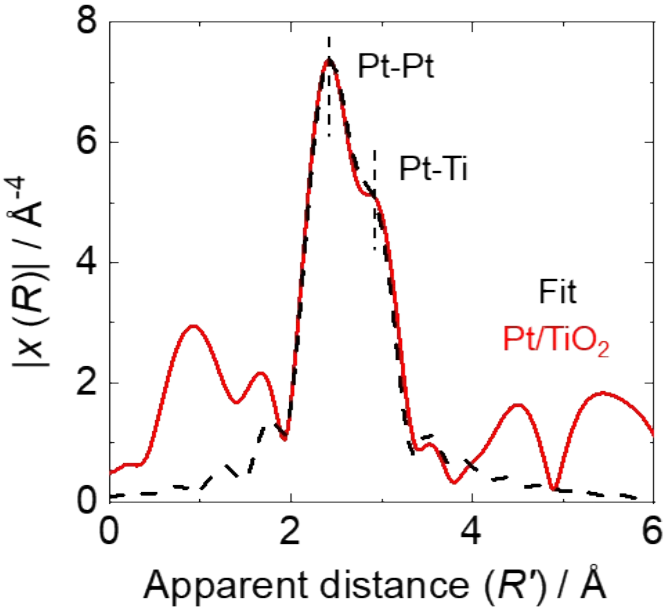

Fig. S5 Results of curve-fitting of FT-EXAFS spectrum ($3 \leq k \leq 10.5$). The dashed line shows the fitting results generated using a crystal structure[8] composed of Pt and Ti. These results indicate that the local structure of the Pt/TiO_2 photocatalyst contained both Pt-Pt and Pt-Ti shells.

Frequency change of CO adsorbed on Pt electrode using in situ CO-probe SEIRAS

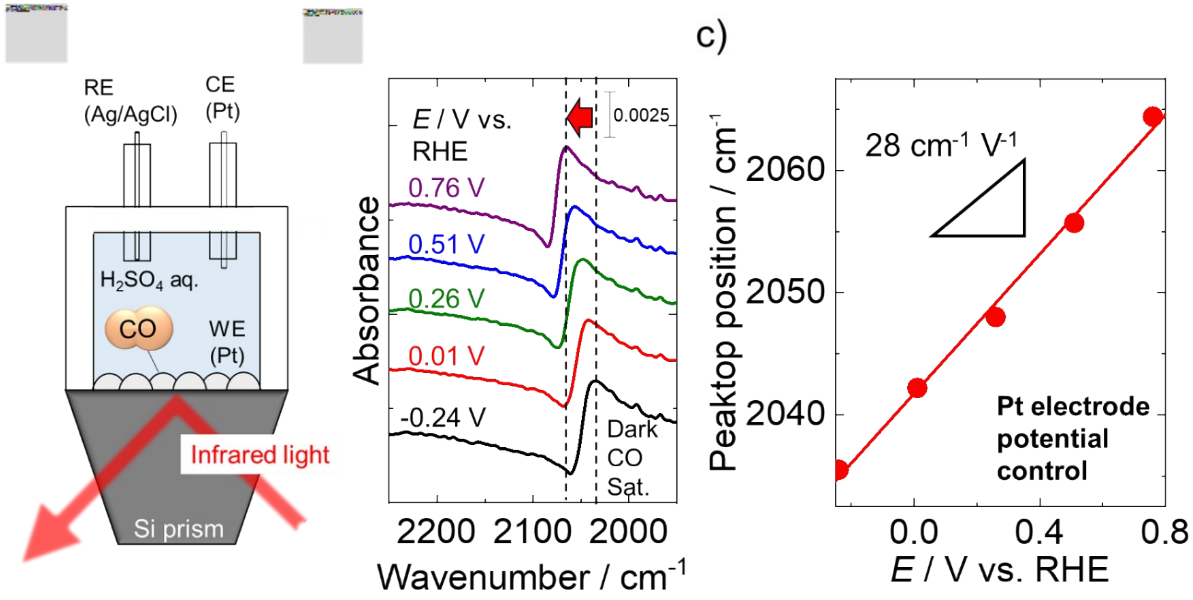

Fig. S6 a) Diagram showing in situ ATR-SEIRAS analysis system using CO molecules as probe on a Pt electrode. The relationship between the potential of the Pt electrode potential and the vibration frequency change of the adsorbed CO was investigated using an electrochemical measurement cell connected to a Pt counter electrode and an Ag/AgCl reference electrode. b) In situ SEIRA spectra of CO adsorbed on Pt electrode at various potentials acquired under dark conditions in CO-saturated 0.05 M aqueous H_2SO_4 solution. c) Peak position in SEIRA spectra as function of applied potential, with slope of 28 cm^{-1} V^{-1}.

Diagram of in situ CO-probe SEIRAS analysis of Pt/TiO_2 photocatalyst

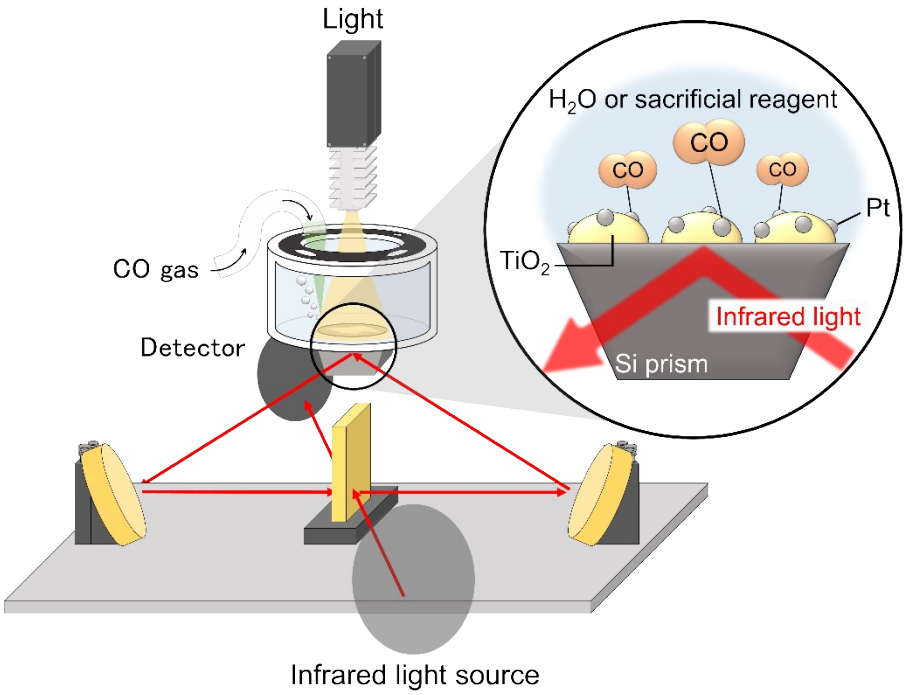

Fig. S7 Diagram of in situ CO-probe SEIRAS process involving light irradiation. The path of the infrared light was directed using gold mirrors to achieve total internal reflection at the interface with a Si prism. The vibration frequency changes of CO molecules adsorbed on Pt particles were tracked during the reaction at steady state where the excited carrier transfer had reached equilibrium.

Electrode potential dependency of adsorbed CO frequency on Pt electrode in neutral solution

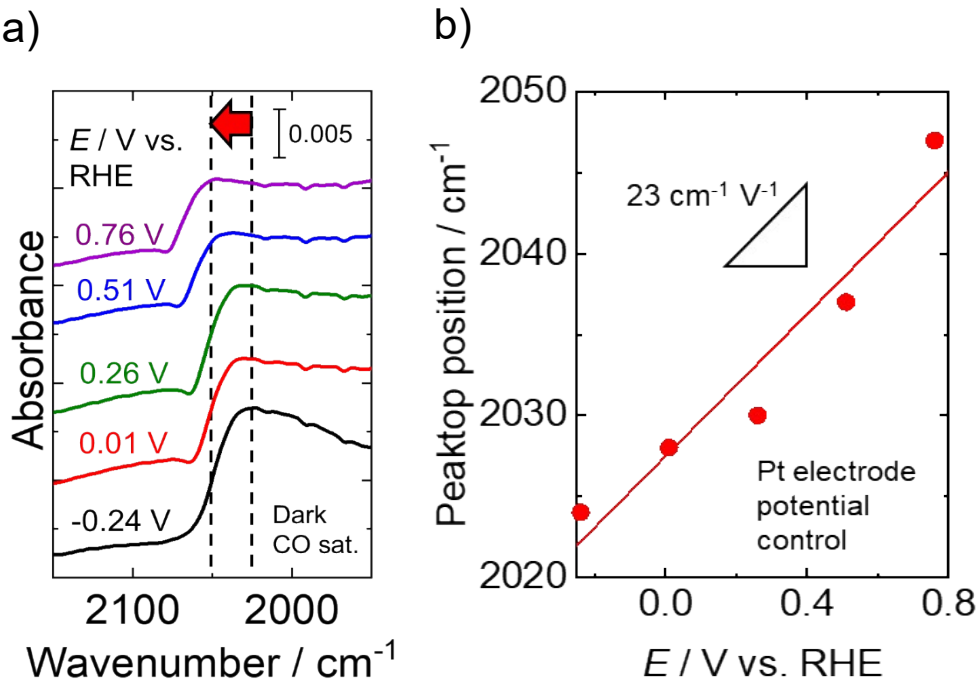

Fig. S8 a) In situ SEIRA spectra of CO adsorbed on Pt electrode at various potentials measured in CO-saturated Na_2SO_4 solution under dark conditions. b) Peak position of SEIRA spectra as a function of applied potential. It should be noted that the SEIRAS measurements of the Pt/TiO_2 photocatalyst in this study utilized the data from H_2SO_4 shown in Fig. S6, because the accuracy of electrochemical control was not enough due to the solution resistance from neutral solution.

Electrode potential dependency of adsorbed CO frequency on Pt/TiO_2 electrode

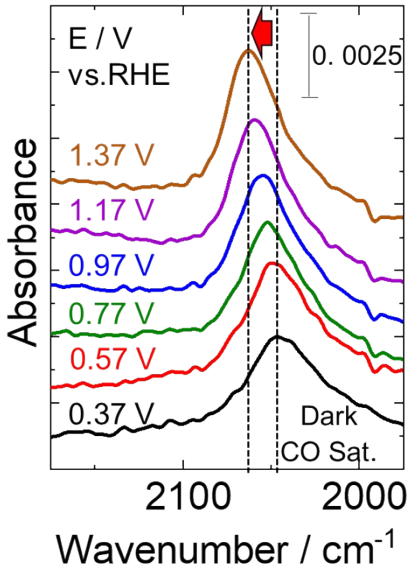

Fig. S9 In situ SEIRA spectra of CO molecules adsorbed on the Pt cocatalyst supported on a TiO_2 photocatalyst (0.5 wt% Pt) at various applied potentials. Measurements were conducted under dark conditions in a CO-saturated 0.1 M aqueous Na_2SO_4 solution. Due to the low conductivity of TiO_2, the numerical voltage applied to the TiO_2 electrode in the graph may not accurately reflect the potential applied to the Pt cocatalyst. This behavior differs from the potential response of the bare Pt electrode shown in Figure S6. Therefore, the local potential changes of the Pt cocatalyst on the TiO_2 photocatalyst were tentatively estimated using the potential-wavenumber relationship of a bare Pt electrode as a calibration curve.

In situ SEIRA spectra of adsorbed CO under dark conditions in different solutions

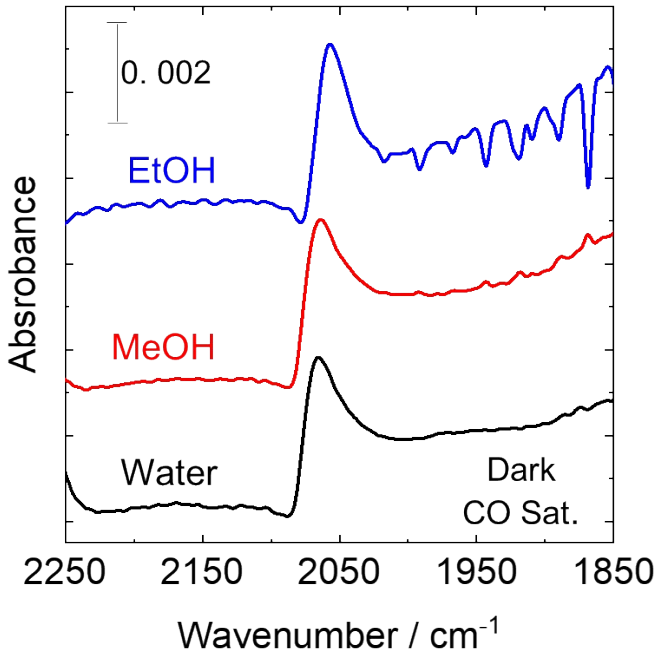

Fig. S10 In situ SEIRA spectra of adsorbed CO under dark conditions in different solutions. The black line represents the spectrum in ultrapure water, while the red and blue lines correspond to spectra in aqueous solutions containing methanol (MeOH) and ethanol (EtOH), respectively. The spectra show negligible differences among the three conditions, indicating that sacrificial reagents such as methanol and ethanol did not influence the SEIRA spectra of CO adsorption on the Pt cocatalyst. This is attributed to the initial adsorption of CO gas onto the Pt cocatalyst using a CO-saturated aqueous solution.

Electrochemical measurements on Pt electrode in N_2 or CO saturated aqueous solution

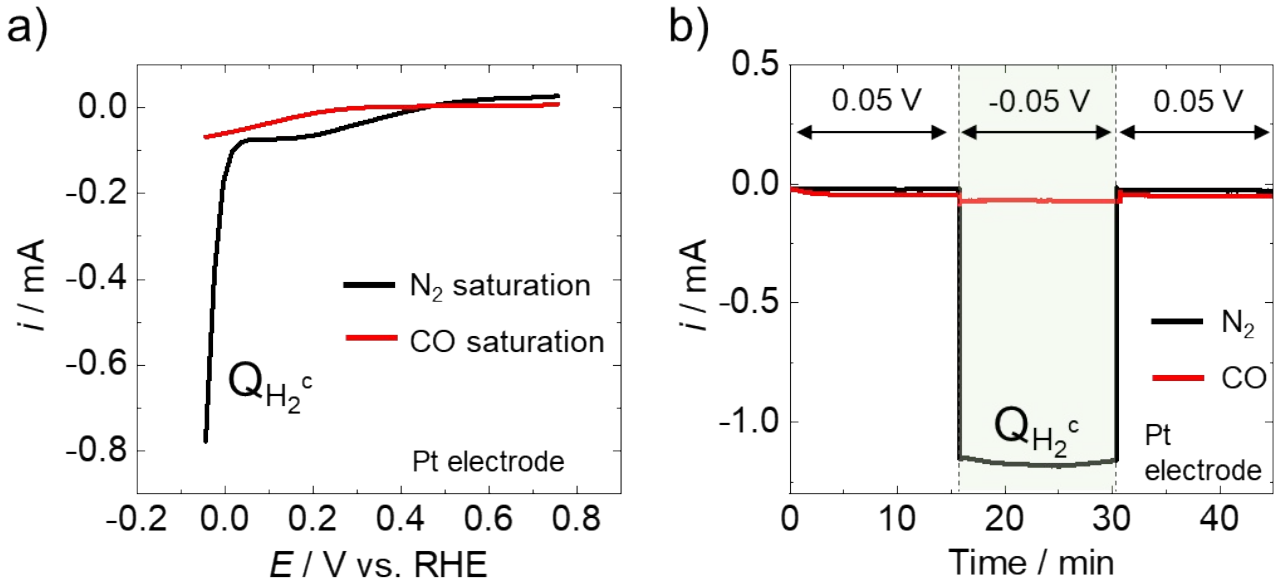

Fig. S11 a) Linear sweep voltammetry (LSV) data obtained by applying potentials from -0.04 V to 0.76 V vs. RHE and b) I-t curve data measured at active (-0.05 V vs RHE) and inactive potentials (0.05 V vs RHE) in 0.1 M H_2SO_4 solution on a Pt electrode. The electrode potential was controlled using a potentiostat. The black and red lines represent the results obtained in N_2-saturated and CO-saturated aqueous solutions, respectively. Q_{H2}^{c} represents the current of hydrogen evolution. The results indicate that there is the possibility that CO may block the hydrogen generation sites on the Pt cocatalyst during SEIRAS measurements, because the CO adsorption prevent electrochemical hydrogen evolution on the Pt electrode.

It should be noted that the suppression of electrochemical hydrogen evolution can be avoided if the Pt-H stretching vibrations[9-10] can be observed by SEIRAS measurements. However, in our system, these signals were not detectable due to their significantly lower intensity, approximately 50 times weaker than that of Pt–CO stretching vibrations. Therefore, we employed adsorbed CO as a probe molecule to sensitively monitor charge transfer to the Pt cocatalyst.

In situ SEIRA spectra of adsorbed CO under different light intensities

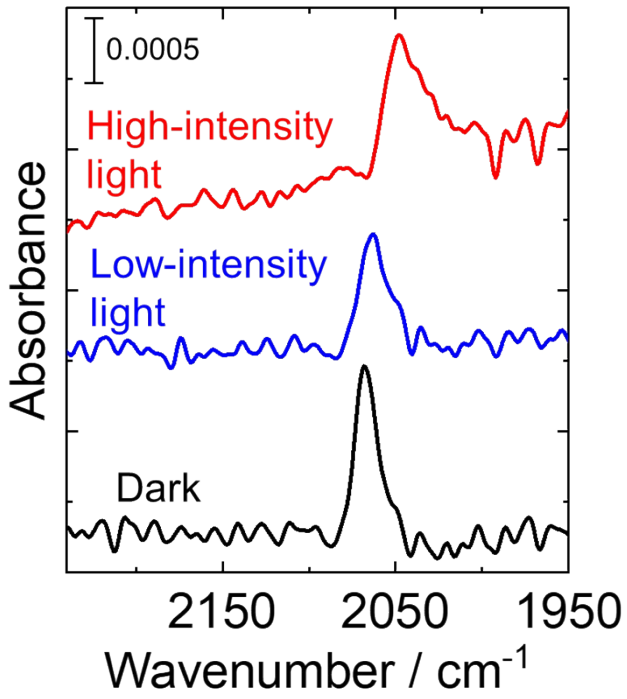

Fig. S12 In situ SEIRA spectra of adsorbed CO under dark condition and high- and low-intensity light irradiation. The black line represents the spectrum under dark conditions, while the red and blue lines correspond to spectra under high- and low-intensity light irradiation, respectively. The spectra show that the magnitude of the shift of the CO peak varies with light intensity, suggesting that the local electrode potential at the Pt cocatalyst is affected by the number of photons absorbed by the photocatalyst.

References

1. S. Tsunekawa, A. Sakai, Y. Tamura, K. Hatada, T. Ina, K.-H. Wang, T. Kawai and M. Yoshida, *Chem. Lett.*, 2022, **51**, 50-53.
2. K.-H. Wang, M. Yoshida, H. Ikeuchi, G. Watanabe, Y.-L. Lee, C.-C. Hu and T. Kawai, *J. Taiwan Inst. Chem. Eng.*, 2020, **110**, 34-40.
3. A. Sakai, K. Harada, S. Tsunekawa, Y. Tamura, M. Ito, K. Hatada, T. Ina, T. Ohara, K.-H. Wang, T. Kawai and M. Yoshida, *Chem. Lett.*, 2022, **51**, 723-727.
4. J. D. Grunwaldt and A. Baiker, *Catal. Lett.*, 2005, **99**, 5-12.
5. B. Ravel and M. Newville, *J. Synchrotron Radiat.*, 2005, **12**, 537-541.
6. B. Ravel, *J. Synchrotron Radiat.*, 2001, **8**, 314-316.
7. M. Newville, *J. Synchrotron Radiat.*, 2001, **8**, 322-324.
8. A. K. Sinha, *Acta Crystallographica Section B Structural Crystallography and Crystal Chemistry*, 1969, **25**, 996-997.
9. K. Kunimatsu, T. Senzaki, G. Samjeské, M. Tsushima and M. Osawa, *Electrochim. Acta*, 2007, **52**, 5715-5724.
10. G. Samjeské, K.-i. Komatsu and M. Osawa, *J. Phys. Chem. C*, 2009, **113**, 10222-10228.